Supporting Information

Unveiling the Critical Role of Strain-Induced Local Structure Changes in Co-N_4 Single-Atom Catalysts for Enhanced Oxygen Reduction and Evolution Reactions

*Yewon Yang, Soyun Lee and Joonhee Kang**

Department of Nano Fusion Technology, Pusan National University, 2 Busandaehak-ro 63-beon-gil, Geumjeong-gu, Busan 46241, Republic of Korea

***E-mail**: j.kang@pusan.ac.kr

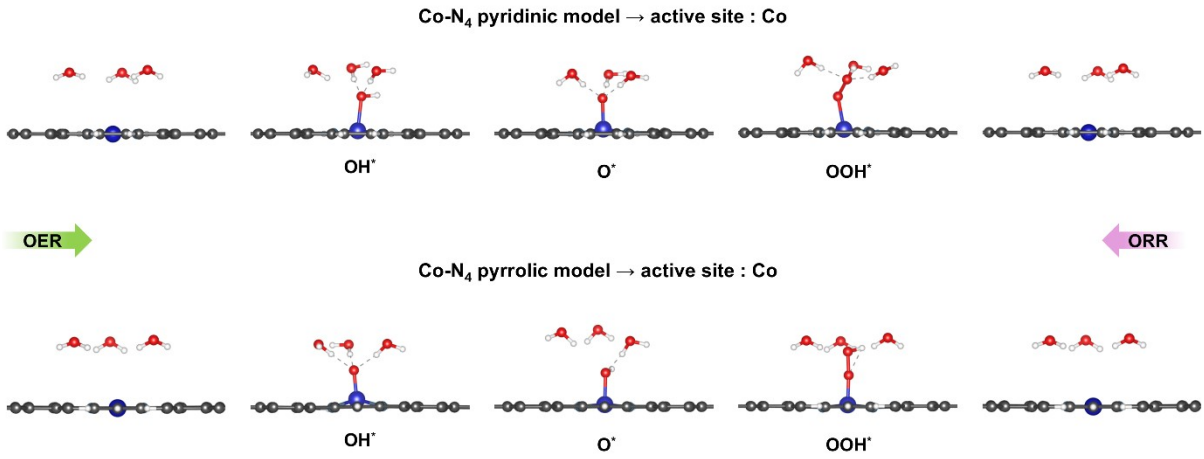

Figure S1. Optimized geometries of Co-N_4 pyridinic and pyrrolic models with three explicitly adsorbed water molecules under VASPsol treatment. The adsorption configurations of key reaction intermediates (OH^*, O^*, and OOH^*) at the Co active site are shown for both OER and ORR processes.

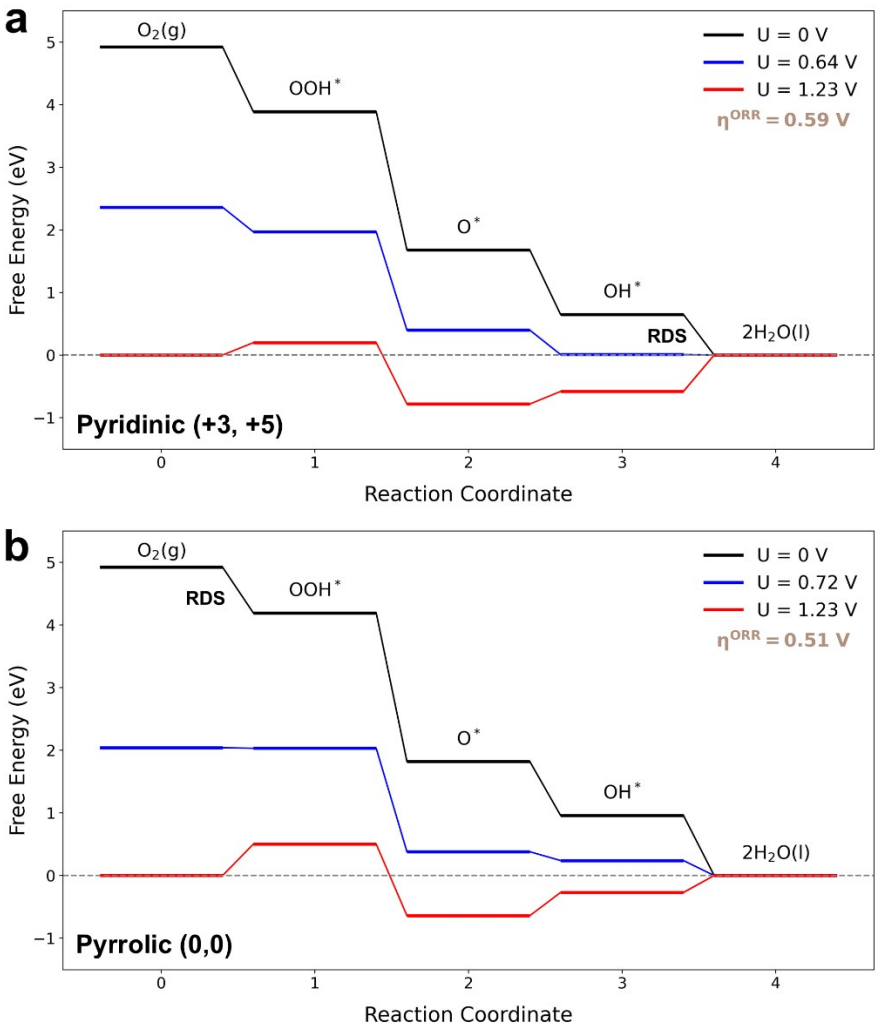

Figure S2. Free energy diagrams of the ORR process on Co-N_4 model systems calculated using VASPsol with explicit adsorption of three water molecules. (a) Pyridinic (+3, +5) and (b) Pyrrolic (0,0)

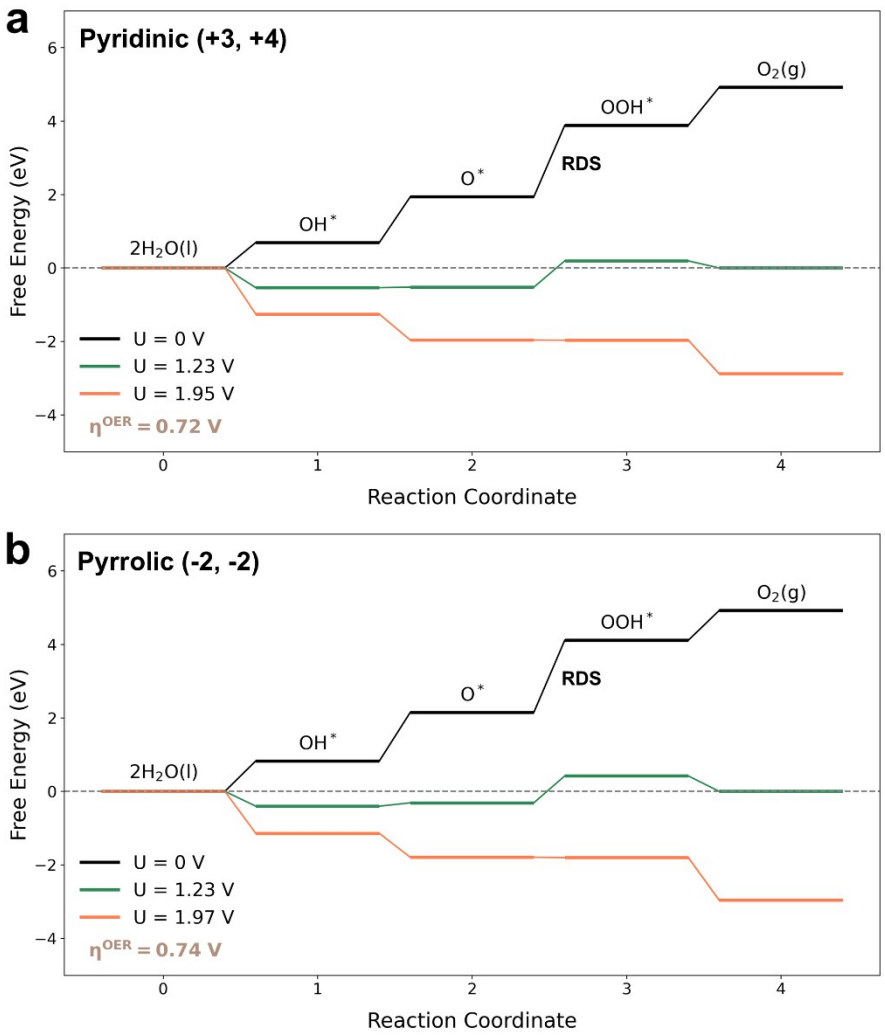

Figure S3. Free energy diagrams of the OER process on Co-N_4 model systems calculated using VASPsol with explicit adsorption of three water molecules. (a) Pyridinic (+3, +4) and (b) Pyrrolic (-2, -2)

Table S1. Zero-point energy and entropy contributions of reaction intermediates and molecules used in free energy calculations.

	ZPE (eV)	TΔS (eV)
H_2O (l)	0.56	0.67 (0.035 bar)
H_2 (g)	0.27	0.41
OH^*	0.36	0
O^*	0.07	0
OOH^*	0.45	0

Table S2. Structural energy variations (eV) of the Co-N_4 pyridinic model under biaxial strain. The energy of the Pyridinic (0,0) is set as the reference (0 eV). Red values highlight the most stable configurations relative to the reference.

	y-axis (eV)						
x-axis (eV)	-3%	-2%	-1%	0%	1%	2%	3%
-3%	32.067	14.513	22.269	20.049	8.844	15.422	30.016
-2%	2.487	1.428	0.700	0.259	0.061	0.131	0.431
-1%	2.042	1.049	0.383	0.003	**-0.131**	-0.010	0.335
0%	1.864	0.934	0.324	**0.000**	-0.083	0.093	0.491
1%	1.969	1.091	0.534	0.257	0.222	0.447	0.888
2%	2.312	1.486	0.977	0.745	0.754	1.018	1.500
3%	2.877	2.105	1.641	1.455	1.499	1.798	2.322

Table S3. Structural energy variations (eV) of the Co-N_4 pyrrolic model under biaxial strain. The energy of the Pyrrolic (0,0) is set as the reference (0 eV). Red values highlight the most stable configurations relative to the reference.

	y-axis (eV)						
x-axis (eV)	-3%	-2%	-1%	0%	1%	2%	3%
-3%	29.323	22.719	18.163	32.760	-0.569	6.565	6.890
-2%	-0.699	-1.088	**-1.181**	-0.993	-0.612	0.015	0.874
-1%	-0.393	-0.745	-0.807	-0.606	-0.195	0.452	1.326
0%	0.143	-0.193	-0.240	**0.000**	0.415	1.080	1.972
1%	0.852	0.545	0.524	0.764	1.217	1.903	2.782
2%	1.753	1.571	1.463	1.717	2.183	2.881	3.771
3%	2.838	2.547	2.560	2.849	3.426	4.001	4.910

Table S4. Calculated adsorption energies (eV) of intermediates (O^*, OH^*, and OOH^*) on the Co-N_4 pyridinic model under different biaxial strain conditions.

Catalysts (Pyridinic)	O^* (eV)	OH^* (eV)	OOH^* (eV)
(0, 0)	2.97	1.37	4.40
(-1, -1)	2.86	1.35	4.35
(-1, +1)	2.97	1.33	4.35
(+3, 0)	2.97	1.37	4.55
(+3, +3)	2.92	1.33	4.37
(+3, +4)	2.40	1.30	4.35
(+3, +5)	2.34	1.28	4.32
(+4, 0)	2.93	1.35	4.53
(+4, +3)	2.36	1.33	4.49
(+4, +4)	2.30	1.30	4.35
(+5, 0)	2.44	1.34	4.49

Table S5. Calculated adsorption energies (eV) of intermediates (O^*, OH^*, and OOH^*) on the Co-N_4 pyrrolic model under different biaxial strain conditions.

Catalysts (Pyrrolic)	O^* (eV)	OH^* (eV)	OOH^* (eV)
(0, 0)	2.28	1.29	4.35
(-1, 0)	2.38	1.39	4.36
(-1, -1)	2.45	1.48	4.37
(-1, -2)	2.53	1.56	4.40
(-1, -3)	2.61	1.22	4.40
(-2, 0)	2.46	1.49	4.37
(-2, -1)	2.54	1.33	4.41
(-2, -2)	2.62	1.66	4.41
(-2, -3)	2.70	1.46	4.40
(+1, 0)	2.00	1.00	4.17
(+2, 0)	2.09	1.08	4.26
(+3, 0)	1.99	0.96	4.25

Table S6. Calculated free energies (G, eV) of intermediates (O^*, OH^*, and OOH^*) on the Co-N_4 pyridinic model under various strain conditions. These values were used to construct the corresponding free energy diagrams for ORR/OER activity analysis.

Catalysts	ΔG_{O^*} (eV)	ΔG_{OH^*} (eV)	ΔG_{OOH^*} (eV)
Pyridinic (0, 0)	2.97	1.06	4.09
Pyridinic (-1, +1)	2.97	1.03	4.05
Pyridinic (+3, 0)	2.96	1.06	4.24
Pyridinic (+3, +3)	2.92	1.03	4.07
Pyridinic (+3, +4)	2.40	1.00	4.04
Pyridinic (+3, +5)	2.33	0.97	4.01
Pyridinic (+4, 0)	2.92	1.04	4.21
Pyridinic (+4, +3)	2.35	1.02	4.19
Pyridinic (+4, +4)	2.29	1.00	4.04
Pyridinic (+5, 0)	2.43	1.04	4.18

Table S7. Calculated free energies (G, eV) of intermediates (O^*, OH^*, and OOH^*) on the Co-N_4 pyrrolic model under various strain conditions. These values were used to construct the corresponding free energy diagrams for ORR/OER activity analysis.

Catalysts	ΔG_{O^*} (eV)	ΔG_{OH^*} (eV)	ΔG_{OOH^*} (eV)
Pyrrolic (0, 0)	2.28	0.99	4.04
Pyrrolic (+1, 0)	1.99	0.69	3.86
Pyrrolic (+2, 0)	2.08	0.78	3.95
Pyrrolic (+3, 0)	1.97	0.66	3.94
Pyrrolic (-1, 0)	2.37	1.09	4.05
Pyrrolic (-1, -1)	2.45	1.18	4.07
Pyrrolic (-1, -2)	2.53	1.26	4.09
Pyrrolic (-1, -3)	2.60	0.92	4.09
Pyrrolic (-2, 0)	2.46	1.18	4.06
Pyrrolic (-2, -1)	2.54	1.02	4.10
Pyrrolic (-2, -2)	2.62	1.13	4.09
Pyrrolic (-2, -3)	2.69	1.16	4.09

Table S8. Calculated N-N bond lengths (Å) of the Co-N_4 pyridinic model under different biaxial strain conditions. The x- and y-axes correspond to the longer (A length) and shorter (B length) N-N bond lengths, respectively.

Catalysts (Pyridinic)	A (Å)	B (Å)
(0, 0)	2.683	2.600
(-1, +1)	2.650	2.617
(+3, 0)	2.798	2.615
(+3, +3)	2.807	2.688
(+3, +4)	2.811	2.709
(+3, +5)	2.813	2.730
(+4, 0)	2.837	2.614
(+4, +3)	2.850	2.690
(+4, +4)	2.853	2.716
(+5, 0)	2.877	2.625

Table S9. Calculated N-N bond lengths (Å) of the Co-N_4 pyrrolic model under different biaxial strain conditions. The x- and y-axes correspond to the longer (A length) and shorter (B length) N-N bond lengths, respectively.

Catalysts (Pyrrolic)	A (Å)	B (Å)
(0, 0)	3.024	2.873
(-1, 0)	3.029	2.802
(-1, -1)	2.998	2.791
(-1, -2)	2.966	2.782
(-1, -3)	2.930	2.769
(-2, 0)	3.037	2.737
(-2, -1)	3.004	2.725
(-2, -2)	2.971	2.716
(-2, -3)	2.938	2.707
(+1, 0)	3.014	2.942
(+2, 0)	3.011	3.009
(+3, 0)	3.082	3.007